Soft Matter

Accepted Manuscript

ROYAL SOCIETY OF CHEMISTRY

www.rsc.org/softmatter

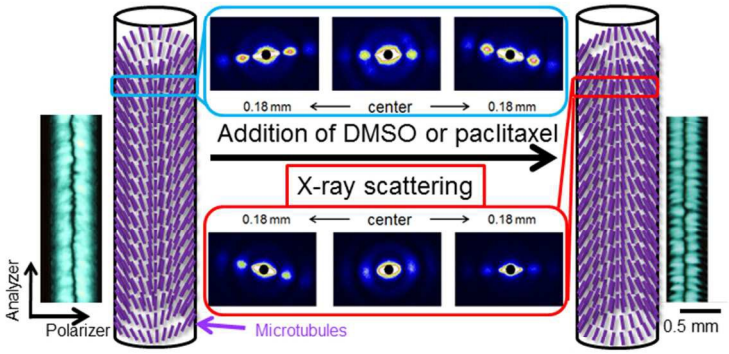

254x190mm (96 x 96 DPI)

Helical Alignment Inversion of Microtubules in Accordance with a Structural Change in Their Lattice

Kazuhiro Shikinaka,[1,*] Saori Mori,[1] Kiyotaka Shigehara,[1] and Hiroyasu Masunaga[2]

[1]Graduate School of Engineering, Tokyo University of Agriculture and Technology, Koganei, Tokyo 184-8588, Japan

[2]Experimental Research Division, SPring-8, Japan Synchrotron Radiation Research Institute, Sayo-ku, Hyogo 679-5198, Japan

RECEIVED DATE (to be automatically inserted after your manuscript is accepted if required according to the journal that you are submitting your paper to)

*To whom correspondence should be addressed: E-mail: k-shiki@cc.tuat.ac.jp (K.S.) Tel./Fax: +81 42-388-7406

RUNNING HEAD: Helical Alignment Inversion of Microtubules

ABSTRACT

Giant helical (oriented chiral nematic) alignments of microtubules of nanometer to centimeter lengths are known to form over a temperature gradient during anisotropic spiral propagation via tubulin dimer addition in a capillary cell. Such helical alignments may be modified by the addition of either paclitaxel or dimethyl sulfoxide, which induces a lattice (helical) structural change in the microtubule itself. In this study, we found that the lattice structural change of microtubules brings about inversion of microtubule alignments in the helical ordering. Based on microscopy and scattering data, a mechanism for the helical ordering of microtubules is discussed in relation to their lattice (helical) structure.

Key words: Microtubules, Hierarchical Ordering, Synchrotron X-ray Scattering

INTRODUCTION

Emerging properties of living organisms reveal well-ordered structures of molecules according to their chirality. The well-organized structure of biomolecules has been studied through their collective movement[1-3] and self-templating assembly[4] under thermodynamic equilibrium conditions. However, the ordered structure of living organisms can be observed under non-equilibrium conditions. Recently, we achieved the formation of centimeter-scale hierarchically regulated alignment of microtubules (MTs) with well-ordered polarity, which resulted from the helical chirality of MTs, by applying non-equilibrium conditions to the MT assembling reaction[5,6].

MTs are rigid, hollow, cylindrical proteins with diameters of approximately 25 nm. MTs are produced via polymerization (*i.e.,* self-assembly) of the globular protein heterodimer tubulin, during which anisotropic spiral addition leads to the assembly of a left-handed helix[7]. To achieve *in vitro* directed propagation of MTs, tubulin solutions have been applied to a confined space over a suitable temperature gradient. Using this experimental setup, well-regulated MT alignments (*i.e.,* an oriented nematic alignment or a giant helical (oriented chiral nematic) alignment) of even-centimeter lengths were achieved by polymerization of tubulins in a long cylindrical/rectangular cell while applying a temperature gradient from a thermostated terminal

(warm terminal) to another (cold) terminal[5,6]; the confined space of the cell enabled temperature regulation.

Because regulated MT alignment occurs through the action of the directed dipole and chiral helicity of MTs[6], a lattice (helical) structural change of an MT may cause transition of the MT helical alignment. In this study, we analyzed the relationship between the transition of the helical alignment of MTs and changes in the lattice structure of an MT after addition of dimethyl sulfoxide (DMSO) or paclitaxel, which affect the lattice structure of MT[8-14]. Using polarized optical microscopy (POM) and synchrotron small-angle X-ray scattering (SAXS), we examined the giant helical alignment of MTs formed in the long capillary cell with either DMSO or paclitaxel over a temperature gradient. Based on the empirical results, we discuss the relationship between the lattice (helical) structure of an MT and the helical alignment of MTs.

RESULTS AND DISCUSSION

The nucleation of tubulin dimers to form oligomers, which are constructed from α and β subunits, is primary event in the assembly of MTs. Because nucleation shows low thermodynamic favorability, a high concentration of tubulin above a specific threshold is required to push the equilibrium in the direction of nucleation. After nucleation, thermodynamically favorable extension of an MT (*i.e.,* polymerization) progresses. The two

terminals of the MTs grow at different velocities: rapid growth onto the "plus" end, which is terminated by a β subunit at the preferential elongation end, and slow growth to the "minus" end, which is terminated by an α subunit[7]. In living organisms, the directional spiral assembly of tubulin dimers onto the plus end is precisely controlled by various binding proteins that also provide signals for subunit addition[15-17]. Therefore, an MT constructed under these principles exhibits inherent polarity along the helical axis, with a plus and minus end. In contrast, regulation *in vitro* by binding protein is less precise, and the assembly of tubulin dimers typically produces imperfect helices that are frequently kinked[18–20]. In addition, MTs exhibit non-hierarchical alignment with random polarity[21,22]. Numerous studies have examined diverse experimental systems to achieve regulated alignment of MTs, typically using microelectromachananical systems[23-27].

As shown in our previous studies[5,6], during preparation of centimeter-scale MT alignments, we constructed a giant helical (oriented chiral nematic) structure under asymmetrical polymerization conditions by applying a temperature gradient to a long capillary glass cell, as described in Figure 1. MT alignments can be observed by microscopy and synchrotron X-ray scattering; previous experiments have revealed the following: 1) nucleation and polymerization of tubulin dimers into MTs occurs irregularly near the warm terminal where the temperature is increased and became constant instantaneously; 2) MTs propagate according to the temperature

gradient from an adequately distant position, where directional propagation or addition of tubulin dimers onto the plus ends of MTs is evident; 3) MTs form regulated ordering along the temperature gradient show oriented alignment on the centimeter scale; 4) observation of anisotropic movements of kinesin, a motor protein that moves on MTs from their minus end to their plus end,[28] along MT filaments showed that the plus ends of MTs were preferentially oriented towards the cold terminal[5]; 5) during the final stage, when MTs were in polymerization/depolymerization equilibrium because of the concentration fluctuations, dynamic rearrangement of MTs such as shrinking (depolymerization), and tilting of the orientation axis, causing a structural change from the oriented nematic alignment to giant helical alignment caused by the ordered dipole and helical chirality of MTs[6].

Because this giant helical alignment results from the helical structure of an MT, the transition of the helical lattice structure of an MT itself may cause a change in the giant helical alignment of MTs. MTs are known to be highly polymeric molecules. In MTs, tubulin dimers bind head-to-tail to form a protofilament (PF). PFs interact laterally to form a cylindrical tube: the MT. MTs with as few as 8 and as many as 19 PFs have been observed *in vivo* and *in vitro*[8,9]. It has also been reported that longitudinal interactions between tubulin dimers in an MT are primarily hydrophobic, and lateral interactions between PFs (*i.e.,* tubulin dimers) in an MT are electrostatic because of the polar interactions between amino acids[10]. The longitudinal

hydrophobic interactions, which are entropy-driven, are affected by the structure of tubulin dimers, which changes with the interactions among tubulin, guanosine triphosphate, and paclitaxel[11]. Lateral electrostatic interactions are influenced by the dielectric constant of the medium; this constant is diminished by the addition of DMSO[12]. In particular, the binding of paclitaxel to the tubulin dimer stabilizes the interaction between dimers in PFs[11]. As a result, in the presence of paclitaxel, tubulin dimers form MTs with a smaller number of PFs relative to the native state[13]. In contrast, addition of DMSO to a tubulin solution makes the native state of the tubulin dimer unfavorable; DMSO enhances the polymerization of tubulin and reduces the surface area per tubulin dimer[12]. Therefore, in the presence of DMSO, tubulin dimers form MTs with a greater number of PFs relative to the native state[14]. This means that the lattice (helical) structure of MTs changes with transitions in the packing of tubulins in an MT[15] after adding DMSO or paclitaxel. The lattice structure of the reconstructed MTs *in vitro* is strongly affected by DMSO and paclitaxel. The helical axis (*i.e.,* the tilt of PFs) of mainly existing MTs in their solution is transformed from the right (an MT with 14 PFs) to the left (an MT with 12 or 15 PFs) relative to the long axis of the MT cylinder after adding DMSO[14] or paclitaxel[13] *in vitro* (Figure 1). In this study, MT alignments formed in the long capillary cell with DMSO or paclitaxel were evaluated over a temperature gradient to determine the relationship between the helical alignment of MTs and the lattice (helical) structure of an MT itself.

POM images were obtained under crossed nicols while changing the angle between the cell and the analyzer (Figures S1–S3) in which the chiral polarity of MTs is likely the source of the giant left-handed helical alignment, as demonstrated previously[6].

As shown in Figure 2a, when the analyzer angle was 0°, the white area was symmetrical in both the left and right halves of the capillary cell, with a dark centerline region after a certain period of evolution. To assess MT alignments, optical retardation was also examined. In the left half of the cell, when the analyzer angle was 0°, counterclockwise tilting of MTs (from the vertical line) was observed because of color subtraction. In contrast, color addition was observed in the right half of the cell; therefore, MTs tilted clockwise from the vertical line. These data agree with the results of previous reports[6].

The addition of either DMSO (Figure 2b) or paclitaxel (Figure 2c) gave rise to distinct domains according to POM images. These domains were divided by a dark centerline region and were stacked in alternate shifts towards the right and left halves of the cell. DMSO and paclitaxel also caused a change in optical retardation in the MT alignments, particularly in the left half of the cell when the analyzer angle was 0°. Because of color addition, we observed clockwise tilting of MTs from the vertical line. In contrast, color subtraction was observed in the right half of the cell; therefore, MTs tilted counterclockwise from the vertical line in the presence of DMSO or paclitaxel. Thus, addition of either DMSO or paclitaxel causes clear

change in MT alignments. Using a narrow and bright synchrotron X-ray source, we performed SAXS experiments on the capillary cell with a 0.5-mm diameter to analyze the structure of MT alignments in accordance with the experimental settings (Figure 3a).

Figure 3b–3d shows SAXS images from the MT alignments 12.5 mm above the warm terminal of the cell for a specific incubation period (see the figure caption). In all scattering images, the central oval scattering pattern assignable to the MT cylinder outer wall scattering patterns and the anisotropic scattering spots near the equatorial line can be distinguished. As shown in Figure 3b, without DMSO and paclitaxel, MT alignments from the centerline point of the cell yielded anisotropic scattering with the tilt angles close to 0° (–2.5°). In contrast, the tilt angles 0.18 mm to the left and 0.18 mm to the right of the centerline point resulted in the production of mirror images, with tilt angles of –7.5° and +12.5° for angles 0.18 mm to the left and 0.18 mm to the right of the centerline point, respectively. This SAXS profile was also obtained in the V-shaped alignments of MT cylinders formed in a rectangular thin glass cell over a temperature gradient, as reported previously[6]. Thus, MTs that are polymerized in a long cylindrical capillary cell with the temperature gradient also form the V-shaped alignments that result in the ordering of giant helical MTs.

In the presence of DMSO or paclitaxel, the scattering patterns resulting from MT alignments at 0.18 mm to the left and 0.18 mm to the right of the centerline (Figure 3c, 3d) appeared to be

mirrored with anisotropic scattering patterns relative to the MT alignments without DMSO or paclitaxel (Figure 3b). These results indicate the inversion of the V-shaped alignments of MT cylinders in the cell after adding DMSO or paclitaxel. As described above, addition of DMSO or paclitaxel to a tubulin solution causes inversion of the tilt direction of the helical axis of an MT itself relative to the long axis of the MT cylinder[13,14]. Therefore, the inversion of the tilt direction of the helical axis in "the MT itself" is expected to cause transition of the V-shaped alignments of MT cylinders in the giant helical ordering of MTs. The prospective illustrations of the MT alignments in the capillary cell obtained from Figure 3b-3d were superimposed on the POM images as Figure S4.

The anisotropic scattering from MT alignments with paclitaxel (Figure 3d) was weaker than that from other samples (Figure 3b and 3c). This may have been caused by the relatively mixed and sparsely settled ordering of MTs corresponding to jumbled optical textures according to POM data (Figure 2c). Acceleration of tubulin dimer nucleation[7] and stabilization of MTs[8] by paclitaxel enables nucleation and growth of tubulin dimers even at low temperatures, such as on the cold side of the long capillary cell. Therefore, the regulation of MT alignment is disrupted by the addition of paclitaxel.

Based on microscopy results and scattering measurements, a schematic representation of the helical alignments of MTs of centimeter length is shown in Figure 4. Tubulin dimers without

either DMSO or paclitaxel form an MT with a left-handed helical structure of tubulins and a right-tilted axis relative to the long axis of the MT cylinder (Figure 4a, right)[13,14]. As a result, over a temperature gradient in the long capillary cell, the tubulins generated a left-handed giant helical structure of MTs with V-shaped alignments (Figure 4a, left); this process generates the chiral polarity of the tubulin helix structure in accordance with previously demonstrated principled shown previously[6].

However, tubulin dimers in the presence of DMSO or paclitaxel form an MT with a left-handed helical structure of tubulins and left-tilted axis relative to the long axis of the MT cylinder (Figure 4b, right)[13,14]. As a result, over a temperature gradient in the long capillary cell, the tubulins generated a left-handed giant helical structure of MTs with their Λ-shaped alignments (Figure 4b, left).

As shown in Figure 4c, the overall left-handed helical structure of MTs was the same regardless of the presence or absence of DMSO or paclitaxel, as shown in the POM images in Figure S1–S3. As shown in the POM images in Figures 2b and 2c, with the similarity of helical filaments consisting of bent-core liquid crystal molecules[29], the Λ-shaped alignments of MTs in the helical structure ensure high integrity of MT alignments in the overall helical structure. Thus, chiral ordering of MTs of centimeter length is transformed by the switching of the lattice structure of an MT of nanometer length.

The results of this study indicate that an adequate confined space, temperature gradient, and specific reagents cause long-range mesoscopic hierarchical ordering of MTs, reflecting the nanoscopic molecular structure of an MT itself, even without regulation by other binding proteins. This is important fact to understand biological systems related to cytoskeletal dynamics, such as emergence and reorganization of long-range MT ordering in plant cells[30,31].

In conclusion, we found that the giant helical alignment of MTs was transformed in accordance with the lattice structure of an MT itself. In a long capillary cell and over a temperature gradient, tubulin dimers formed the giant helical alignment of MTs, which is caused by the ordered dipole and helical chirality of tubulins in an MT. The helical alignment of MTs transformed into a more strongly integrated structure in the overall helical structure resulting from changes in the packing of MTs, in accordance with the transition of the lattice (helical) structure of an MT itself. Our results offer new insights into the fine regulation of molecular ordering of cytoskeletal proteins and its relationship with molecular structure. The structural ordering of chiral biomolecule such as MT, rod-like viruses, and DNA has been studied by many researchers[21,22,32-36]. The presented structural control of chiral MT architecture here also exhibits distinct correspondence between the uniform macroscopic ordering of biomolecules and the microscopic chiral structure in biomolecule itself.

The control of hierarchical ordering of cytoskeletal proteins has been demonstrated by arranging proteins with the help of a molecular motor, both experimentally and theoretically[1-3]. Because a motor is not involved in the ordering proposed in the present study, our experimental system can describe the role of structure in cytoskeletal protein assembly and ordering. Furthermore, based on our results, the mesoscale hierarchical ordering of molecular assemblies is finely dictated by the nanoscale organization of cytoskeletal dimer proteins.

EXPERIMENTAL

Tubulin purification. Tubulin was purified according to Castoldi et al[37]. from porcine brains using concentrated 1,4-piperazinediethanesulfonate (PIPES) buffer[37]. The high-concentration PIPES buffer and Brinkley BR buffer 1980 (BRB80) were prepared using the dipotassium salt of PIPES (Sigma Aldrich, St. Louis, MO, USA), and the pH was adjusted by adding HCl solution. The purity of obtained tubulin was judged to be 98–99% by Coomassie blue staining of proteins that had been separated in overloaded (50 μg per lane) sodium dodecyl sulfate/polyacrylamide electrophoresis minigels.

Formation of MT alignments in a long capillary cell under a precise temperature gradient. The procedures were conducted as described previously[6]. To obtain MT alignments, tubulin dimer solutions were polymerized in a cylindrical capillary cell (0.5-mm diameter ×

30-mm length of the inner space with wall thickness of 0.2 mm; Mito Rika-Glass K.K., Mito, Japan) over a temperature gradient along the cell's long axis (Figure 1). Approximately 12 μL of a BRB80 buffer solution containing 1.0 mM GTP and 380 μM tubulin dimers with or without 3.0 w/v% DMSO or 1.0 μM paclitaxel was inserted into the cell, in which one terminal was heated by placing it on thin cover glass attached on a thermostated plate set to 37 °C (FP900, Mettler Toledo GmbH, Greifensee, Switzerland).

POM measurements. The samples were examined using POM (BX51, Olympus, Tokyo, Japan) equipped with a CCD camera (Olympus). To examine optical retardation, a 530-nm sensitive color plate (U-TP530, Olympus) was set between the sample and the analyzer.

SAXS. MT alignment experiments were carried out using the BL45XU SPring-8 beam line (Hyogo, Japan), which was equipped with a double-crystal silicon monochromator. Energy of the X-rays was 14.0 keV; the beam size was 0.034 × 0.032 mm^2; wavelength 0.10 nm. Scattering pattern images at the various points on sample were obtained at a frame size of 487 × 195 pixels and 172 × 172 μm^2 using the PILATUS 100K detector system (Swiss Light Source [SLS]). The q range covered in the SAXS measurement was 0.08–4.00 nm^{-1}, where $q = 4\pi \sin(\theta/2)/\lambda$ and θ was the scattering angle. The photon flux of the X-ray source, exposure time, and specimen-to-detector distance were 4.8 × 10^{10} photons/(s·mm^2), 3 s, and 2.06 m,

respectively. Denaturation of MTs or MT alignments was never confirmed, even during continuous irradiation of X-ray for 300 s in the SAXS measurements.

ASSOCIATED CONTENT

Supporting Information Available

Time-lapse POM images of the MT alignments. This material is available at free of charge via the Internet at http://pubs.acs.org

AUTHOR INFORMATION

Corresponding Author

Telephone/Fax: +81-42-388-7406. E-mail: k-shiki@cc.tuat.ac.jp.

Notes

The authors declare no competing financial interest.

ACKNOWLEDGMENTS

We thank Mr. Keisuke Kaneda, Mr. Hiroki Kudoh, and Prof. Hiromitsu Moriyama (Tokyo University of Agriculture and Technology) for their assistance with the tubulin purification and

SAXS measurements. This study was supported by the Moritani Scholarship Foundation. The synchrotron irradiation experiments were performed at BL45XU in SPring-8 with the approval of the Japan Synchrotron Radiation Research Institute (JASRI; Proposal No. 2011B1406).

REFERENCES

(1) T. Surrey, F. Nédélec, S. Leibler and E. Karsenti, Physical properties determining self-organization of motors and microtubules. *Science* 2001, **292,** 1167-1171.

(2) V. Schaller, C. Weber, C. Semmrich, E. Frey and A. R. Bausch, Polar patterns of driven filaments. *Nature* 2010, **467,** 73-77.

(3) T. B. Liverpool and C. Marchetti, Instabilities of isotropic solutions of active polar filaments. *Phys. Rev. Lett.* 2003, **90,** 138102.

(4) (a) W.-J. Chung, J.-W. Oh, K. Kwak, B. Y. Lee, J. Meyer, E. Wang, A. Hexemer and S.-W. Lee, Biomimetic self-templating supramolecular structures. *Nature* 2011, **478,** 364-368; (b) T. Gibaud, E. Barry, M. J. Zakhary, M. Henglin, A. Ward, Y. Yang, C. Berciu, R. Oldenbourg, M. F. Hagan, D. Nicastro, R. B. Meyer and Z. Dogic, Reconfigurable self-assembly through chiral control of interfacial tension. *Nature* 2012, **481,** 348–351.

(5) A. Kakugo, Y. Tamura, K. Shikinaka, M. Yoshida, R. Kawamura, H. Furukawa, Y. Osada and J. P. Gong, Formation of well-oriented microtubules with preferential polarity in a confined space under a temperature gradient. *J. Am. Chem. Soc*. 2009, **131,** 18089–18095.

(6) K. Shigehara, H. Kudoh, S. Mori, Y. Tamura, A. Kakugo, R. Kawamura, H. Furukawa, J. P. Gong, H. Masunaga, T. Masui, S. Koizumi and K. Shikinaka, Nematic growth of microtubules that changed into giant spiral structure through partial depolymerization and subsequent dynamic ordering. *Soft Matter* 2012, **8,** 11544-11551.

(7) H. Lodish, A. Berk, C. A. Kaiser, M. Krieger, M. P. Scott, A. Bretscher, H. Ploegh and P. T. Matsudaira, *Molecular Cell Biology*, W.H. Freeman & Co. Ltd., San Francisco, CA, 4th edn., 1999.

(8) S. Ray, E. Meyhöfer, R. A. Milligan and J. Howard, Kinesin follows the microtubule's protofilament axis. *J. Cell Biol.* 1993, **121,** 1083-1093.

(9) L. A. Amos and J. Löwe, How Taxol® stabilises microtubule structure. *Chem. Biol.* 1999, **6,** R65-R69.

(10) E. Nogales, M. Whittaker, R. A. Milligan and K. H. Downing, High-resolution model of the microtubule. *Cell* 1999, **96,** 79-88.

(11) G. M. Alushin, G. C. Lander, E. H. Kellogg, R. Zhang, D. Baker and E. Nogales, High-Resolution Microtubule Structures Reveal the Structural Transitions in αβ-Tubulin upon GTP Hydrolysis. *Cell* 2014, **157,** 1117-1129.

(12) T. Arakawa, Y. Lita and S. N. Timasheff, Protein precipitation and denaturation by dimethyl sulfoxide. *Biophys. Chem.* 2007, **131,** 62-70.

(13) J. F. Díaz, J. M. Valpluesta, JP. Chacón, G. Diakun and J. M. Andreu, Changes in microtubule protofilament number induced by taxol binding to an easily accessible site. *J. Biol. Chem.* 1998, **273,** 33803-33810.

(14) A. Kakugo, A. Md. R. Kabir, N. Hosoda, K. Shikinaka and J. P. Gong, Controlled clockwise–counterclockwise motion of the ring-shaped microtubules assembly. *Biomacromolecules* 2011, **12,** 3394-3399.

(15) L. A. Amos, Microtubule structure and its stabilisation. *Org. Biomol. Chem.* 2004, **2,** 2153-2160.

(16) K. Kurokawa, T. Nakamura, K. Aoki and M. Matsuda, Mechanism and role of localized activation of Rho-family GTPases in growth factor-stimulated fibroblasts and neuronal cells. *Biochem. Soc. Trans*. 2005, **33,** 631-634.

(17) T. M. Svitkina and G. G. Borisy, Arp2/3 complex and actin depolymerizing factor/cofilin in dendritic organization and treadmilling of actin filament array in lamellipodia. *J. Cell. Biol*. 1999, **145,** 1009-1026.

(18) D. Chretien and R. H. Wade, New data on the microtubule surface lattice. *Biol. Cell.* 1991, **71,** 161-174.

(19) D. Chretien and S. D. Fuller, Microtubules switch occasionally into unfavorable configurations during elongation. *J. Mol. Biol.* 2000, **298,** 663-676.

(20) J. Howard, *Mechanism of Motor Proteins and the Cytoskeleton*, Sinauer Assoc. Inc., Sunderland, Massachusetts, USA, 2001.

(21) J. Tabony and D. Job, Spatial structures in microtubular solutions requiring a sustained energy source. *Nature* 1990, **346,** 448-451.

(22) J. Tabony, Morphological bifurcations involving reaction-diffusion processes during microtubule formation. *Science* 1994, **264,** 245-248.

(23) Y. Hiratsuka, T. Tada, K. Oiwa, T. Kanayama and T. Q. P. Uyeda, Controlling the direction of kinesin-driven microtubule movements along microlithographic tracks. *Biophys. J.* 2001, **81,** 1555-1561.

(24) R. K. Stracke, J. Böhm, L. Wollweber, J. A. Tuszynski and E. Unger, Analysis of the migration behaviour of single microtubules in electric fields. *Biochem. Biophys. Res. Commun.* 2002, **293,** 602-609.

(25) T. B. Brown and W. O. Hancock, A polarized microtubule array for kinesin-powered nanoscale assembly and force generation. *Nano Lett.* 2002, **2,** 1131-1135.

(26) Y.-M. Huang, M. Uppalapati, W. O. Hancock and T. N. Jackson, Microtubule transport, concentration and alignment in enclosed microfluidic channels. *Biomed. Microdevices* 2007, **9,** 175-184.

(27) M. Uppalapati, Y.-M. Huang, T. N. Jackson and W. O. Hancock, Microtubule alignment and manipulation using AC electrokinetics. *Small* 2008, **4,** 1371-1381.

(28) J. Howard, A. J. Hudspeth and R. D. Vale, Movement of microtubules by single kinesin molecules. *Nature* 1989, **342,** 154-158.

(29) K. Sakai, R. Sakurai and H. Nohira, New resolution technologies controlled by chiral discrimination mechanisms. *Top Curr. Chem.* 2007, **269,** 199-231.

(30) X.-Q. Shi, Y.-Q. Ma, Understanding phase behavior of plant cell cortex microtubule organization. *Proc. Nat. Acad. Sci. USA* 2010, **107,** 11709-11714.

(31) Y. Oda and H. Fukuda, Secondary cell wall patterning during xylem differentation. *Curr. Opin. Plant Biol.* 2012, **15,** 38-44.

(32) S. Bonazzi, M. Capobianco, M. M. D. Morais, A. Garbesi, G. Gottarelli, P. Mariani, M. Grazia, P. Bossi, G. P. Spada and L. Tondelli, Four-Stranded Aggregates of Oligodeoxyguanylates Forming Lyotropic Liquid Crystal: A Study by Circular Dichroism Optical Microscopy, and X-ray Diffraction. *J. Am. Chem. Soc.* 1991, **113,** 5809-5816.

(33) F. Tombolato, A. Ferrarini and E. Grelet, Chiral Nematic Phase of Suspensions of Rodlike Viruses: Left-Handed Phase Helicity from a Right-Handed Molecular Helix. *Phys. Rev. Lett.* 2006, **96,** 258302.

(34) S. Tomar, M. M. Green and L. A. Day, DNA-Protein Interactions as the Source of Large-Length Scale Chirality Evident in the Liquid Crystal Behavior of Filamentous Bacteriophages. *J. Am. Chem. Soc.* 2007, **129,** 3367-3375.

(35) E. Barry, D. Beller and Z. Dogic, A model liquid crystalline system based on rodlike viruses with variable chirality and persistence length. *Soft Matter* 2009, **5,** 2563-2570.

(36) G. Zanchetta, F. Giavazzi, M. Nakata, M. Buscaglia, R. Cerbino, N. A. Clark and T. Bellini, Right-handed double-helix ultrashort DNA yields chiral nematic phases with both right- and left-handed director twist. *Proc. Nat. Acad. Sci. USA* 2010, **107,** 17497-17502.

(37) M. Castoldi and A. V. Popov, Purification of brain tubulin through two cycles of polymerization–depolymerization in a high-molarity buffer. *Prot. Expr. Purif.* 2003, **32,** 83-88.

Figure Captions

Figure 1. (left) Schematic illustration of the experimental system of MT polymerization in the longwise cylindrical capillary cell over a temperature gradient. (right) Anticipated structure of MTs in the presence of both DMSO and paclitaxel.

Figure 2. POM images and optical retardation of the MT alignments in the long capillary cell over a temperature gradient in the absence of DMSO and paclitaxel (a; after 180 min of incubation), in the presence of 3.0 w/v% DMSO (b; after 180 min of incubation), and in the presence of 1.0 μM paclitaxel (c; after 480 min of incubation). The angle between the cell and the analyzer is illustrated on the right. The arrows A and P represent the analyzer and polarizer directions. The warm terminal of each cell was the bottom side.

Figure 3. (a) Illustration of the experimental setup of SAXS measurement. (b–d) SAXS images from the MT alignments in the long capillary cell with a temperature gradient in the absence of DMSO and paclitaxel (a; after 180 min of incubation), in the presence of 3.0 w/v% DMSO (b; after 180 min of incubation), and in the presence of 1.0 μM paclitaxel (c; after 480 min of incubation). SAXS measurements were performed 12.5 mm above the warm terminal on three observation spots as shown in (a).

Figure 4. Prospective illustration of the giant helical alignment of MTs (a) without DMSO and paclitaxel and (b) with either DMSO or paclitaxel. The detailed structure of MTs in the alignment is described on the right side of each illustration. (c) The pattern diagram of the helical structure in the MT alignments.

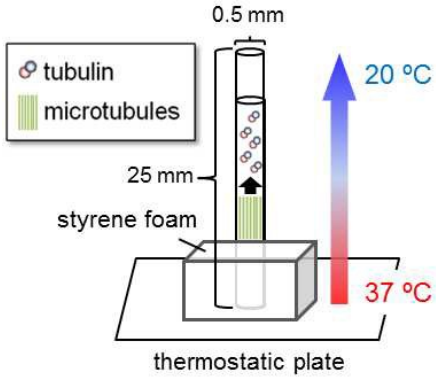

	Number of PF	Tilt angle of PF*	Helicity of MT
Pristine	14	+0.54	Left-handed
+ DMSO	15	-0.98	Left-handed
+ paclitaxel	12	-1.74	Left-handed

*Ref. 19; clockwise tilting against long axis of MT corresponds to positive

Figure 1. Shikinaka et al.

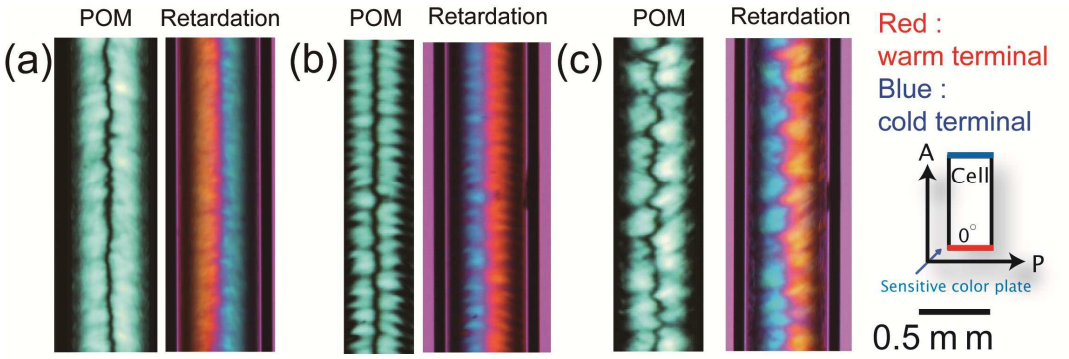

Figure 2. Shikinaka et al.

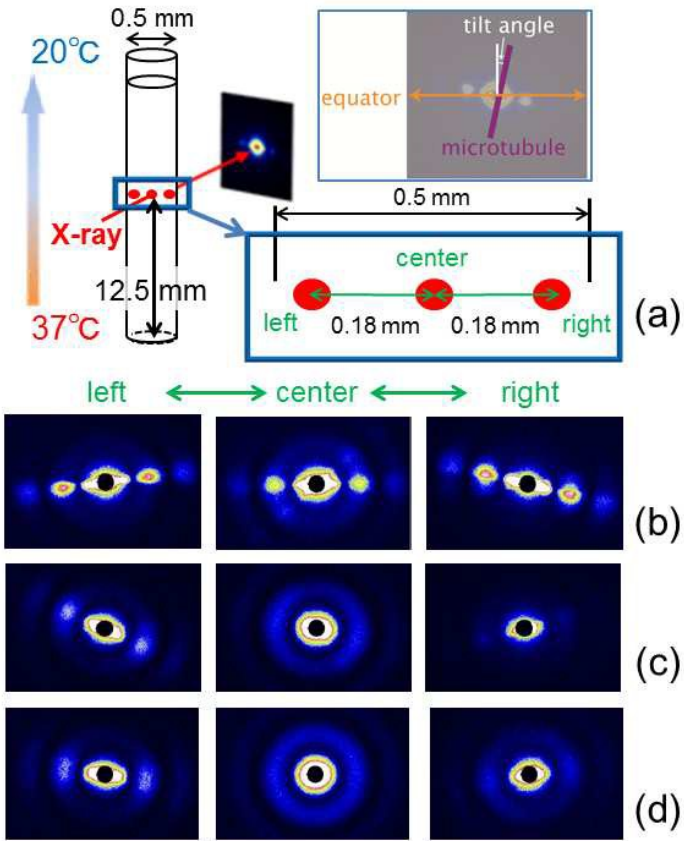

Figure 3. Shikinaka et al.

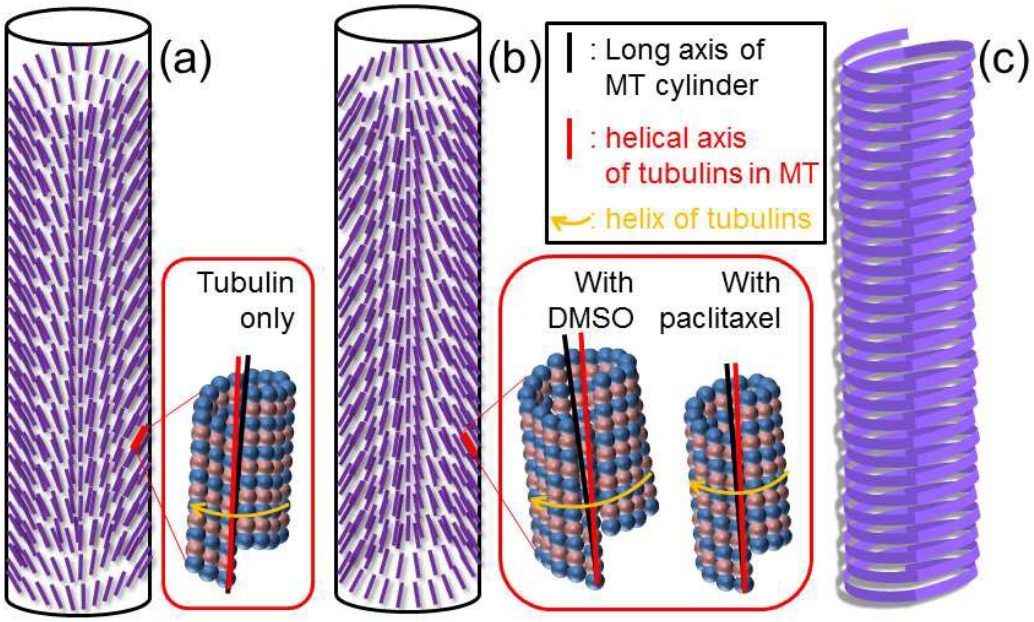

Figure 4. Shikinaka et al.